HTML ABSTRACT + LINKS

Experimental analysis of the quasi-Fermi level split in quantum dot intermediate-band solar cells

A. Luque, A. Martí, N. López, E. Antolín, and E. Cánovas
Instituto de Energía Solar, Escuela Técnica Superior de Ingenieros de Telecomunicación, Universidad Politécnica de Madrid, Ciudad Universitaria sn, 28040 Madrid, Spain

C. Stanley and C. Farmer
Department of Electronics and Electrical Engineering, University of Glasgow, Glasgow, G12 8QQ, United Kingdom

L. J. Caballero
Instituto de Energía Solar, Escuela Técnica Superior de Ingenieros de Telecomunicación, Universidad Politécnica de Madrid, Ciudad Universitaria sn, 28040 Madrid, Spain

L. Cuadra
Departamento de Teoría de la Señal y Comunicaciones, Escuela Politécnica Superior, Universidad de Alcalá, Campus Universitario, 28871 Alcalá de Henares, Madrid, Spain

J. L. Balenzategui
Centro de Investigaciones Energéticas, Medioambientales y Tecnológicas–Departamento de Energías Renovables, CIEMAT-DER, Avd. Complutense 22, Madrid 2804, Spain

(Received 22 February 2005; accepted 7 July 2005; published online 17 August 2005)

The intermediate-band solar cell (IBSC) has been proposed as a device whose conversion efficiency can exceed the 40.7% limiting value of single-gap cells. It utilizes the so-called intermediate-band material, characterized by the existence of a band that splits an otherwise conventional semiconductor bandgap into two sub-bandgaps. Two important criteria for its operation are that the carrier populations in the conduction, valence, and intermediate-bands are each described by their own quasi-Fermi levels, and that photocurrent is produced when the cell is illuminated with below-bandgap-energy photons. IBSC prototypes have been manufactured from InAs quantum dot structures and analyzed by electroluminescence and quantum efficiency measurements. We present evidence to show that the two main operating principles required of the IBSC are fulfilled. © *2005 American Institute of Physics*. [DOI: 10.1063/1.2034090]

The prospect of intermediate levels being used to increase the current generated by solar cells was acknowledged many years ago.[1] Calculations have shown that impurity levels may have beneficial although marginal effects[2] and it has been proved experimentally that multiple layers of quantum wells[3] enhance the photocurrent. The intermediate-band solar cell (IBSC) concept proposed in Ref. 4 provides new insight into the conversion efficiencies of solar cells, and offers a potential way to increase the limiting efficiency of a single gap cell from 40.7% to 63.2%, by overcoming the difficulty of increasing the solar cell photocurrent without degrading its voltage.

The basic structure[5] of an IBSC is shown in Fig. 1. It consists of p and n semiconductor layers sandwiching the so-called intermediate-band (IB) material. The electronic structure of this IB material is similar to that of a traditional semiconductor but is characterized by the existence of an additional intermediate-band within the normal bandgap E_G, splitting it in two with energies E_L and E_H.

The theory underpinning the operation of the cell predicts that when illuminated, photons are able to pump electrons from (i) the valence band (VB) to the conduction band (CB), (ii) the VB to the IB, and (iii) the IB to the CB (processes labelled as "1", "2", and "3", respectively, in Fig. 1). In this way, current is enhanced when compared with that of a single energy gap solar cell since low energy photons can now contribute to current generation. In an ideal device, in order to make photon absorption processes "2" and "3" possible, the IB needs to be half-filled with electrons since both electrons and empty states are required to supply electrons to the CB as well as accepting them from the VB. This is also due to the fact that the energy bandwidth of the IB has to be as narrow as possible.[6] A narrow IB also leads to a high effective mass and a low carrier mobility that makes carrier transport within the band difficult. By enabling both photon absorption processes "2" and "3" possible in the same spatial location, no transport is required through the IB. In practical devices, this condition can be relaxed when transport through the IB for short distances is permitted.

However, photocurrent enhancement alone does not suffice to improve the efficiency of a solar cell if the output voltage is not preserved. In this respect, the IBSC theory

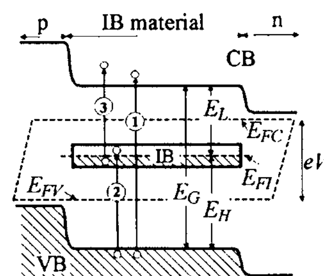

FIG. 1. Band structure of an IBSC, showing transitions, energy gaps, and quasi-Fermi levels.

 © 2005 American Institute of Physics

	Layer
	5 nm 10^{19} cm^{-3} p^+ Be-Al$_{0.8}$Ga$_{0.1}$As
	100 nm 10^{19} cm^{-3} p^+ Be-GaAs
	200 nm 2×10^{18} cm^{-3} p Be-GaAs
	5 nm un-GaAs
	4×10^{10} cm^{-2} Si δ-doped layer
	5 nm un-GaAs
10x	2.7 ML InAs (QDs)
10x	5 nm un-GaAs
10x	4×10^{10} cm^{-2} Si δ-doped layer
10x	5 nm un-GaAs
	300 nm 2×10^{17} cm^{-3} n Si-GaAs
	100 nm 2×10^{18} cm^{-3} n^+ Si-GaAs
	2×10^{17} cm^{-3} n-GaAs substrate

FIG. 2. Epitaxial layer structure of the IBSC based on InAs quantum dots embedded in GaAs.

predicts that the carrier concentration in each band is described by its own quasi-Fermi level: E_{FC} for the CB, E_{FI} for the IB, and E_{FV} for the VB. The output voltage of the IBSC, V, is then determined by the quasi-Fermi level split between electrons (E_{FC}) and holes (E_{FV}) as shown in Fig. 1. This voltage is, therefore, limited by the largest of the bandgaps involved, E_G, and not by either of the smaller ones (E_L and E_H).

Quantum dots (QDs) have been proposed as a practical means of realizing IB material,[7] where the IB would arise from the confined electronic states in the dots. QDs are preferred over other low-dimensional structures such as quantum wires or wells, because dots provide a true zero density of states between the IB and the CB preventing the easy de-excitation of electrons from the CB to the IB and favoring a split of the quasi-Fermi levels between the CB and the IB.

QD solar cells prototypes have been fabricated by standard III-V semiconductor processing from stacked layers of self-organized InAs quantum dots embedded in GaAs barrier material, and grown by molecular beam epitaxy in the Stranski–Krastanov[8] growth mode. Their general layer structure is shown in Fig. 2 and will be referred to as samples of type A. These samples have a δ-doping layer inbetween each quantum dot layer with the aim of supplying electrons to half-fill the IB[9] by modulation doping. Equivalent structures, but with the δ-doping layers omitted were also grown: they will be referred to as samples of type B. Finally, another set of samples was grown, named R (reference) and lacking both QDs and δ-doping layers.

The quantum efficiency (number of electrons produced as photocurrent per incident photon of a given wavelength) of the samples was measured; representative results are plotted in Fig. 3. Quantum dot solar cells of type A and B show production of photocurrent when illuminated with below bandgap-energy photons ($\lambda > 900$ nm) while samples without QDs do not. The physical origin of this photocurrent is interpreted as follows: photons with energy higher than E_H (Fig. 1) are able to pump electrons from the VB to the IB. These electrons are then extracted as photocurrent when they become thermally pumped from the IB to the CB.

The electroluminescence (number of photons per unit of time emitted when cells are forwarded biased) was also measured. Results are shown in Fig. 4. The biasing current was 5 A cm^{-2} (cell area is 0.16 cm^{-2}). The theory describing the emission of photons from the IB solar cells has been investigated elsewhere.[5,10] It is found that the spectral distribution

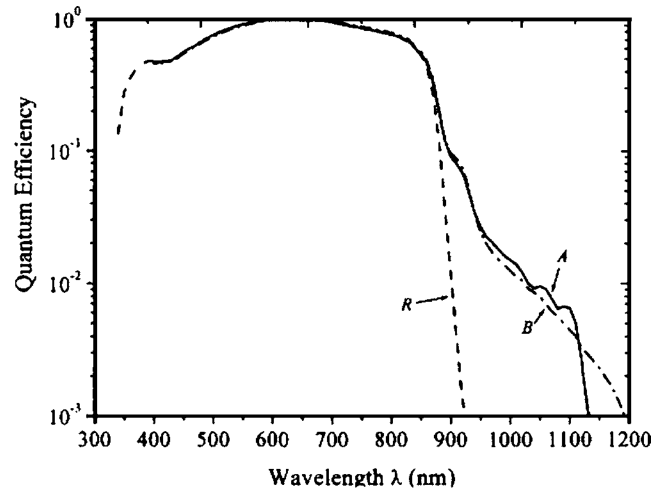

FIG. 3. Quantum efficiency of the quantum dot-based IBSCs. "R" labels the GaAs reference, "A" is the sample with both QDs and δ-doped layers while "B" is the sample with QDs but lacking the δ-doped layers.

of the electroluminescent photon flux emitted by the front side of the cell, and associated with radiative recombination of electrons from the IB to the VB, is given by

$$\frac{dN_{ph}^{IV}}{d\varepsilon} = \frac{2\pi \exp(\mu_{IV}/kT) a(\varepsilon, W_{IB}) \alpha_{IV} \exp(-\varepsilon/kT)\varepsilon^2(1-R)}{h^3c^2(\alpha_{CV}+\alpha_{IV}+\alpha_{CI})}, \tag{1}$$

where α_{XY} is the absorption coefficient (cm^{-1}) of the Y-band$\rightarrow$X-band transition, R is the surface reflectivity, ε is the photon energy and $\mu_{XY}=E_{FX}-E_{FY}$ is the split between quasi-Fermi levels E_{FX} and E_{FY}. In addition, the absorbance $a(\varepsilon, W_{IB})$, is given by

$$a(\varepsilon, W_{IB}) = 1 - \exp[-(\alpha_{CV}+\alpha_{IV}+\alpha_{CI})W_{IB}] \tag{2}$$

where W_{IB} is the thickness of the intermediate-band material which in our case is the region containing the dots. The rest of the symbols have been defined or have their usual meanings.

The spectral distribution of photons emitted as a result of CB to VB transitions follows a similar law to the one written

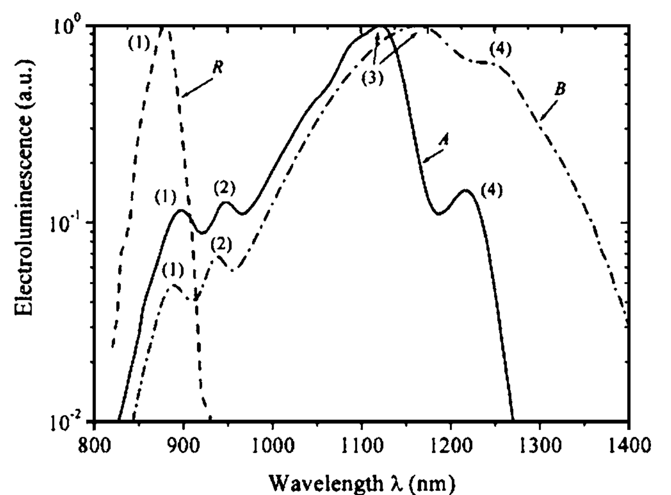

FIG. 4. Electroluminescence of the quantum dot IBSCs. "R" labels the GaAs reference, "A" the sample with both QDs and δ-doped layers, and "B" the sample with QDs but with the δ-doped layer omitted. The numbers "1" to "4" identify the different peaks.

TABLE I. Experimental data for the determination of μ_{CI}.

Sample type	ε_3(eV)(nm) (nm)	ε_1(eV) (nm)	$QE(\varepsilon_3)/QE(\varepsilon_1)$	R^{ph}_{CVIV}	μ_{CI}(eV)
A	1.107	1.378	0.00267/0.0906	0.115/1	0.112
	1120	900			
B	1.064	1.393	0.00185/0.1263	0.489/1	0.187
	1165	890			

in Eq. (1) for an ideal device, but with the absorption coefficients changed to their appropriate counterparts. Neglecting photons produced by means of CB to VB transitions that are reabsorbed through transitions from the IB to the CB and from the VB to the IB, the spectral distribution for the photons caused by CB to VB transitions is approximated by

$$\frac{dN^{CV}_{ph}}{d\varepsilon} = \frac{2\pi \exp(\mu_{CV}/kT) a(\varepsilon, W) \exp(-\varepsilon/kT)\varepsilon^2(1-R)}{h^3c^2}, \quad (3)$$

where W is now the total thickness of the device.

Several peaks appear in the electroluminescence spectra in Fig. 4. Comparing the emission spectrum from the IB cell with that from the GaAs reference cell, we associate peak "1" with the gallium arsenide signature. Peak "2" is most likely due to the existence of a wetting layer or to a higher energy bound state in the quantum dots. Peaks "3" and "4" are associated with deep confined electron energy states of in the dots. We will take peak "3" as representative of the energy levels introduced by the dots. Calculations below will not change significantly if peak "4" is assumed instead.

As can be seen from Eqs. (1) and (3), the light emitted from the cells under forward bias contains valuable information about the quasi-Fermi level split μ_{IV}, μ_{CV} and therefore μ_{CI} since $\mu_{CI}=\mu_{CV}-\mu_{IV}$. However, this information is not easy to extract due to the difficulty of measuring the fluxes described by Eqs. (1) and (2) in absolute terms. Conversely, measurement of the ratio between two electroluminescence peaks is more easily done. Using Eqs. (1) and (3), the ratio, R^{ph}_{CVIV}, for the peaks corresponding to the CB$\rightarrow$VB and IB $\rightarrow$VB transitions, is given by

$$R^{ph}_{CVIV} = \exp\left[\frac{\mu_{CI}}{kT}\right]\exp\left[-\frac{\varepsilon_1-\varepsilon_3}{kT}\right]\frac{a(\varepsilon_1, W)\varepsilon_1^2\{1-R(\varepsilon_1)\}}{a(\varepsilon_3, W_{IB})\alpha_{XY}/\{\alpha_{CV}(\varepsilon_3)+\alpha_{IV}(\varepsilon_3)+\alpha_{CI}(\varepsilon_3)\}\varepsilon_3^2\{1-R(\varepsilon_3)\}}, \quad (4)$$

where ε_1 and ε_3 are the energies of the electroluminescence peaks represented in Fig. 4.

Applying the same model framework to the one above used to describe emission, the quantum efficiency (QE) for the two energies of interest is given by

$$QE(\varepsilon_3) = a(\varepsilon_3, W_{IB})\frac{\alpha_{IV}(\varepsilon_3)\{1-R(\varepsilon_3)\}}{\alpha_{CV}(\varepsilon_3)+\alpha_{IV}(\varepsilon_3)+\alpha_{CI}(\varepsilon_3)}, \quad (5)$$

$$QE(\varepsilon_1) = a(\varepsilon_1, W)\{1-R(\varepsilon_1)\}. \quad (6)$$

Substituting these values into Eq. (4) we obtain

$$\mu_{CI} = kT\ln\left(R^{ph}_{CVIV}\frac{\varepsilon_3^2 QE(\varepsilon_3)}{\varepsilon_1^2 QE(\varepsilon_1)}\exp\left(\frac{\varepsilon_1-\varepsilon_3}{kT}\right)\right). \quad (7)$$

This equation allows the experimental determination of the splitting of the CB and IB quasi-Fermi levels. The data to be used in Eq. (7), obtained from Figs. 3 and 4, is summarized in Table I, and leads to a value μ_{CI}=0.187 and 0.279 eV for samples A and B respectively.

In summary, we have presented experimental evidence to support both the production of photocurrent from below bandgap-energy photons as well as the existence of three separated quasi-Fermi levels associated with the CB, the IB, and the VB of an IB quantum dot solar cell structure. The results have been based on the combined spectral analysis of the quantum efficiency and electroluminescence of the cells.

It appears that the introduction of the δ-doping layers has little or no influence on the quasi-Fermi level split between the CB and the IB. It is also possible that each emission peak is best described by its own individual quasi-Fermi level so that a generalized description of the phenomena would require the introduction of more than the three quasi-Fermi levels assumed here.

This work has been supported by the FULLSPECTRUM project, funded by the European Commission under Contract No. SES6-CT-2003-502620, the Spanish Plan for R&D (TIC2003-02281), and the Comunidad de Madrid (GR/MAT/0075/2004). One of the authors (E.C.) acknowledges the "Plan Nacional de Formación de Personal Investigador" research grant. The authors also want to thank W. Reid, J. C. Zamorano and J. Piñero for their assistance with the experimental set-ups.

[1] M. Wolf, Proc. IRE **48** 1246 (1960).
[2] M. J. Keevers and M. A. Green, J. Appl. Phys. **78**(8), 4022 (1994).
[3] K. W. Barnham and G. Duggan, J. Appl. Phys. **67**, 3490 (1990).
[4] A. Luque and A. Martí, Phys. Rev. Lett. **78**, 5014 (1997).
[5] A. Luque and A. Martí, Prog. Photovoltaics **9**, 73 (2001).
[6] L. Cuadra, A. Martí and A. Luque, *Proceedings of the 16th European Photovoltaic Solar Energy Conference* (James and James, London, 2000), p. 15.
[7] A. Martí, L. Cuadra, and A. Luque, Proc. 28th IEEE PVSC, Anchorage, (IEEE; New York), 940 (2000).
[8] Y. Nakata, Y. Sugiyama, and M. Sugawara, Semicond. Semimetals **60**, Chap. 2 (1999).
[9] A. Martí, L. Cuadra, and A. Luque, IEEE Trans. Electron Devices **48**, 2394 (2001).
[10] L. Cuadra, A. Martí, and A. Luque, IEEE Trans. Electron Devices **51**, 1002 (2004).

Applied Physics Letters is copyrighted by the American Institute of Physics (AIP). Redistribution of journal material is subject to the AIP online journal license and/or AIP copyright. For more information, see http://ojps.aip.org/aplo/aplcr.jsp